processes

MDPI

Article

Reverse Osmosis Modeling Study of Lead and Arsenic Removal from Drinking Water in Tarija and La Paz, Bolivia

Esteban Manuel Villena-Martínez [1,2,*], Paola Andrea Alvizuri-Tintaya [2,3], Jaime Lora-García [4], Juan Ignacio Torregrosa-López [4] and Vanesa Gladys Lo-Iacono-Ferreira [2]

1 Departamento de Ingeniería y Ciencias Exactas, Universidad Católica Boliviana "San Pablo", Tarija, Bolivia
2 Project Management, Innovation and Sustainability Research Center (PRINS), Universitat Politècnica de València, Alcoy Campus, Plaza Ferrándiz y Carbonell, s/n, E-03690 Alcoy, Spain
3 Centro de Investigación en Agua, Energía y Sostenibilidad, Universidad Católica Boliviana "San Pablo", La Paz, Bolivia
4 Research Institute for Industrial, Radiophysical and Environmental Safety (ISIRYM), Universitat Politècnica de València, Plaza Ferrándiz y Carbonell, s/n, E-03690 Alcoy, Spain
* Correspondence: evillena@ucb.edu.bo

Abstract: An investigation of primary water sources in two Bolivian basins identified the presence of heavy metals toxic to health that exceeded the permissible limits for drinking water. Lead deposited in the San Jacinto and Huacata–Tarija reservoirs within the Guadalquivir basin and arsenic in the Milluni–La Paz basin were identified. The work studies reverse osmosis (RO) to remove Pb and As. The main contribution of this research is the development and construction of a mathematical model based on the Spiegler–Kedem concentration polarization model using different concentrations of Pb and As. The model makes it possible to design high conversion facilities (>80%) and optimize the process from the point of view of energy efficiency in future works. The model was developed to also include an Arrhenius temperature adjustment factor that allows for an accurate prediction of the process performance. The experimentation was carried out in two RO pilot plants using polyamide membranes. The model fits correctly with a maximum relative error between the experimental and theoretical flows of 5.4% and 4.4%. Among the benefits of the study, it guarantees the rejection of metals greater than 99%, even at low pressures.

Keywords: heavy metals; safe water; reverse osmosis; concentration polarization; mathematical model; temperature correction

Citation: Villena-Martínez, E.M.; Alvizuri-Tintaya, P.A.; Lora-García, J.; Torregrosa-López, J.I.; Lo-Iacono-Ferreira, V.G. Reverse Osmosis Modeling Study of Lead and Arsenic Removal from Drinking Water in Tarija and La Paz, Bolivia. *Processes* **2022**, *10*, 1889. https://doi.org/10.3390/pr10091889

Academic Editors: Ana Catarina Sousa and Sónia Días Coelho

Received: 12 August 2022
Accepted: 13 September 2022
Published: 17 September 2022

1. Introduction

The increase in pollution due to different anthropogenic activities has resulted in the reduction of potable water sources in different parts of the world [1–3]. Bolivia, a country located in the heart of South America, is one of these locations. Increased population growth coupled with poorly controlled development has led to a growing and sustained process of water pollution in various areas of the country [4,5]. The Milluni and Guadalquivir basins are important in Bolivia because they are the sources of drinking water for two large cities in the country, La Paz and Tarija. Both basins are currently contaminated with toxic heavy metals, which represents a risk to the public health and safety of the population [6–8]. Not many studies exist that determine the origin of arsenic and lead in water sources in either the Milluni or Guadalquivir basins. The Swiss cooperation study [9] identifies that mining is one of the main polluting factors of water in the Milluni basin. Medina et al. [10] indicate that agrochemical misuse is one of the factors in the contamination of the San Jacinto reservoir of Tarija.

Some heavy metals such as copper, zinc, manganese, iron, and cobalt play an essential role in the biochemical processes of the human body. However, excessive exposure to these metal ions can cause hazardous impacts. Other heavy metals such as arsenic,

cadmium, lead, mercury, and chromium are toxic, even at trace levels, because they can accumulate in the human body [11]. Not only do they pose a risk to public health, but toxic metal contaminants also pose a challenge for developing and applying effective water treatments [12].

Recent studies show that membrane filtration technology includes promising processes for drinking water treatment and recovery [13–16]. One membrane filtration process that has attracted particular attention in recent years is reverse osmosis (RO) [17–19]. RO has become an essential tool for industrial applications and is undergoing further research to orient this process towards sustainability [20]. Fritzmann et al. [21] point out that RO is a mature and widely used technology worldwide for desalination, purification, and water recovery.

However, the concentration polarization (CP) process results in a higher solute concentration near the membrane, thus decreasing membrane permeability [22]. In addition, membrane fouling occurs with CP. Both conditions cause lower permeation at a given feed pressure. The result is an increase in energy consumption [19,23–26] and a reduction in process performance, operation, sustainability, and economic viability.

When the CP effect in an RO system occurs, the solute tends to accumulate on the surface of the membrane so that there is a high flux of flow through the membrane but a lower flux of solutes. Solutes that do not pass through the membrane are entrained in the rejection stream since the flow velocity through the membrane is low. The solutes can only pass into the bulk of the rejection stream by back-diffusion in the opposite direction to the permeate flow. At a steady state, the net flux of the solute passing through the liquid film equals the solute flux through the membrane. The solute concentration increases in a boundary layer, reaching its maximum value at the membrane surface [27,28].

The concentration of solutes on the surface of the membrane is a function of the balance of convective forces carrying the solute towards the membrane and diffusive forces causing the solute to return to the bulk solution. In essence, the CP results in the solute being retained in the adjacent zone of the membrane in a transitory manner and, unlike fouling, may cease to exist when the driving force ceases [25]. This CP effect results in a concentrated solution on the approach side of the membrane but not after passing through the membrane [29].

Developing a mathematical model that adequately expresses the RO process's performance is essential for optimizing cost reduction in the final design and implementation of the system [30]. Several mathematical models have described mass transfer and hydrodynamic permeability in RO systems. The specific research topic in the mass transfer is the CP-dominated process near the membrane. Modeling this process is necessary to predict RO separation [16].

The physical and chemical interaction between different feed components and the membrane surface in the CP process is complex. One method to predict membrane performance and pumping energy requirements is quantifying the CP process by choosing between several mass transfer correlations [20,31–34].

The coupling between a mass transfer correlation for CP and the solute transport in the membrane, as described by the Spiegler–Kedem model, requires the simultaneous evaluation of the following three parameters: the Stavermann reflection coefficient σ, solute permeability L_p, and mass transfer coefficient k_m. The variable speed method, which provides information on the reflection coefficient and permeability of the solute, can be helpful in fitting the mentioned coupled model [35].

Al–Obaidi et al. [36] developed a two-dimensional mathematical model to separate dilute aqueous solutions by RO that can be used to predict and analyze the flow, pressure, concentration, and temperature in the membrane. This would facilitate the estimation of water flow and solute concentration. The model is validated using experimental data that simulates the process under steady-state conditions to gain a deeper insight into the process. The results indicate that the development of the model allows the operating parameters to be estimated and the impact of the concentration, pressure, and temperature on the

solution's physical properties to be analyzed, taking into account the varied coefficient of mass transfer and the concentration polarization. The research shows the importance of developing mathematical models to evaluate the RO, which in our case, applies to the separation of heavy metals such as Pb and As.

Temperature is difficult to control in a natural environment and can greatly affect the speed of transport. Therefore, it is essential to evaluate its effect on RO operation [37]. Transport through dense films can be viewed as an activated process usually represented by an Arrhenius-type equation [38].

Alanod et al. [39] propose a device-adapted mathematical model that enables energy recovery in an RO system. It evaluates the effects with various process operating conditions, including the feed rate, pressure, and temperature. The simulation results showed that the total energy consumption could be reduced at a low flow rate and feed pressure and with high values of temperature. These considerations have been used for the present work.

Abejon et al. [40] demonstrated the technical and economic feasibility of removing As through an optimized reverse osmosis process, with the optimization strategy's total cost minimization as the objective. In addition, Ning et al. [41] also indicated that RO effectively removes arsenic in its highest oxidation state. Schimdt et al. [42] studied the separation of arsenic on a pilot scale in groundwater. Both aerated and non-aerated water was considered, although higher removal levels were achieved in aerated water. However, working in an anoxic mode, international water standards were not met [42].

Some research shows that the elimination of As reaches rejection rates higher than 95%. However, they highlight the need to further investigate the separation of heavy metals in drinking water [41,43–46].

Schjeniter and Middlebrooks [47] in their research show the reduction of arsenium and fluoride concentrations in groundwater were reduced by between 60% and 90% from almost 80 µg/L. Fluoride concentrations were reduced by approximately 60% from nearly 1.7 mg/L. Likewise, Kang et al. [48] point out that pH control in As removal with RO may be more successful. Akin [49] investigated As removal with SW and BW-30 membranes (FILMTEC). The results confirm that the rejection increases with the increase in the operating pressure and that it also depends on the type of membrane. Research on the rejection of arsenic in water by RO is important for the development of this work.

This research demonstrates the effect of concentration polarization on the behavior of reverse osmosis membranes in the separation of lead and arsenic in drinking water. The experimental phase was carried out with controlled water solutions in the laboratory with different concentrations of lead and arsenic combined with sodium chloride. NaCL allows for the simulation of the presence of other contaminants in natural water. The main contribution of this research is the development and construction of a mathematical model based on the Spiegler–Kedem [50,51] concentration polarization model using different concentrations of Pb and As. The model allows for the design of high conversion facilities (>80%) and optimizes the process from the point of view of energy efficiency in future works. The model has been developed including an Arrhenius temperature adjustment factor that allows an accurate prediction of the process performance. The model was validated with the experimental results obtained in two RO pilot plants on two campuses of the Universidad Católica Boliviana San Pablo.

The results show that the operation of the RO at low pressures is effective in the rejection of Pb and As in drinking water, allowing energy savings without affecting the physical behavior of the membrane. The current research is an important contribution to guarantee safe water to the population in a sustainable way.

Study Zone

The Milluni and Guadalquivir basins comprise important natural sources of drinking water for the municipalities of La Paz and Tarija, Figure 1. Therefore, during 2018 and 2019, within the framework of a doctoral research project with the Technological University of Valencia, monitoring was carried out to determine the quality of water resources in

the study basins. The results of the study showed the presence of harmful heavy metals and metalloids with concentrations that exceeded the permissible limits of the Bolivian regulations [8,52]. The main problem was lead and arsenic, for which Bolivian regulations state a maximum acceptable limit is 0.01 mg/L [50]. Lead and arsenic concentrations were 50% and 44% higher than this limit. Expecting to have at least 94% rejection of contaminants.

Monitoring of the reservoirs of San Jacinto and Huacata in Tarija and Milluni in La Paz was performed. Concentrations of Pb and As were much higher than those specified in the regulations. The Bolivian Standard establishes a maximum admissible parameter of 0.01 mg/L for Pb and As [53]. The follow-up study showed the presence of other multivalent ions in the water.

Figure 1. Location of the Guadalquivir and Milluni basins.

RO is a method that stands out for its high separation selectivity and high efficiency to guarantee safe water for human consumption. In 2019 and 2020, two experimental pilot plants were installed on the Tarija and La Paz campuses of the Bolivian Catholic University to investigate and evaluate the separation process of inorganic contaminants in water by RO [8].

The proposed experiment considers the evaluation of the RO process to separate lead and arsenic in synthetic waters combined with sodium chloride, in concentrations representative of those found during the monitoring work [8].

2. Model Theory

A schematic of the phenomenon of CP demonstrating the increased concentration in the feed boundary layer due to the retention of solute is shown in Figure 2. At distances from the wall greater than the boundary layer thickness δ, the concentration C_f takes the value of the bulk feed solution because the flow tangential to the membrane is assumed to be turbulent. In the CP boundary layer, the concentration gradually increases until reaching a maximum at the membrane surface C'_f because of the convective flow toward the membrane wall. If there is no complete retention of the solute, some amount of the solute passes through the membrane, causing the permeate concentration C_p.

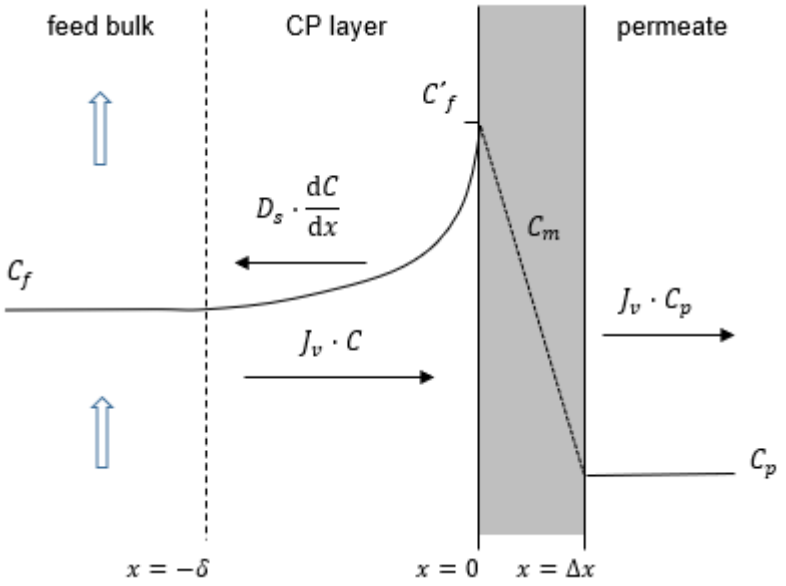

Figure 2. Concentration polarization in the membrane boundary layer.

The Spiegler–Kedem model [50,51] is based on the principles of irreversible thermodynamics. It relates the fluxes of the solvent and solute with the coefficients of transport, which in turn are independent of solute concentration [54]. For a system made up of two components, water and solute, the expression of the volumetric flux and the intrinsic retention for this model are:

$$J_v = L_p \cdot (\Delta P - \sigma \cdot \Delta\pi) \quad (1)$$

$$R_m = 1 - \frac{1-\sigma}{1-\sigma \cdot \exp\left(-(1-\sigma) \cdot \frac{J_v}{B_s}\right)} \quad (2)$$

where:

J_v: volumetric flux;
L_p: water permeability of the membrane;
ΔP: transmembrane pressure;
$\Delta\pi$: difference in osmotic pressure;
Σ: reflection coefficient;
B_s: solute transport coefficient;
R_m: intrinsic salt rejection index of the solute.

For a solute, the observed salt rejection index R_o and the intrinsic salt rejection R_m are calculated using the solute concentration in the bulk or the solute concentration at the feed membrane wall C'_f and the solute concentration in the permeate side C_p.

$$R_o = \frac{C_f - C_p}{C_f} \quad (3)$$

$$R_m = \frac{C_f - C_p}{C_f} \quad (4)$$

In the boundary layer, the balance between convective flow in the fee, back-diffusion, and convective flows that will pass to the permeate gives:

$$J_v \cdot C_p = J_v . C - D_s \cdot \frac{dC}{dx} \quad (5)$$

where:

C: solute concentration in the CP layer;

D_s: diffusion coefficient of the solute.

The integration of the concentration gradient from Equation (5) along the boundary layer with the boundary conditions given by the solute concentration in the bulk solution and solute concentration at the membrane wall yields results in:

$$\frac{C_f - C_p}{C_f - C_p} = \exp\left(\frac{J_v\,\delta}{D_s}\right) = \exp\left(\frac{J_v}{k}\right). \quad (6)$$

where the mass transfer coefficient, k, can be obtained from a mass transfer correlation based on Reynolds and Schmidt numbers, or also as a result of fitting Equation (11) to the experimental data. In this work, the latter has been chosen due to the difficulty of using a wide range of input velocities to the membrane module, limited by the characteristics of the pilot plant.

The average volumetric flux of permeate is calculated using the effective area of the membrane, S, as:

$$J_v = \frac{Q_p}{S} \quad (7)$$

According to Equations (3), (4) and (6), the observed and intrinsic rejections are related by the following equation:

$$\frac{Rm\ (1 - Ro)}{Ro\ (1 - Rm)} = \exp\left(\frac{J_v}{k}\right) \quad (8)$$

The difference in osmotic pressure between both membranes sides is:

$$\Delta\pi\ = R_g \cdot T \cdot (C_f - C_p) \quad (9)$$

where:

R_g: perfect gas law constant;

T: absolute temperature.

The dependence of the permeability parameter on temperature is modeled by an Arrhenius-type equation [38]:

$$L_p(T) = L_{p,0} \cdot \exp\left(-\frac{\Delta H}{R_g} \cdot \left(\frac{1}{T} - \frac{1}{T_0}\right)\right) \quad (10)$$

The value of $-\Delta H/R_g$ fitted to membrane permeability results in different temperatures. The model considers a reference temperature of T_0 = 293 K [8].

Combining Equations (6), (9) and (10) with Equation (1), we obtain the temperature-dependent model for the volumetric flux based on total solute concentration:

$$J_v(T) = L_p(T) \cdot \left[\Delta P\ - \sigma \cdot R_g \cdot T \cdot (C_f - C_p) \cdot \exp\left(\frac{J_v}{k}\right)\right] \quad (11)$$

Note that in the case of a solution containing a major solute and minority ions, Equation (10) is applicable to the main solute which is responsible for most of the osmotic pressure.

The observed rejection of a minority solute (i) is related to the volumetric flux by Equation (12) which is obtained by the combination of Equations (2)–(4) and (6).

$$\frac{R_{o,i}}{1 - R_{o,i}} = \frac{\sigma}{1 - \sigma} \cdot \left[1 - \exp\left(-\frac{J_v(T) \cdot (1 - \sigma)}{B_{s,i}}\right)\right] \cdot \exp\left(-\frac{J_v(T)}{k_i}\right) \quad (12)$$

3. Materials and Methods

This section describes the water problems of the study areas and the previous work carried out for the research, such as the monitoring of the water sources and the assembly of the pilot RO plants for the research. In addition, the characteristics of the membrane

and chemicals used are detailed, and the model used for the analysis of the CP and the proposed adjustment of the model are described, incorporating the temperature adjustment as a key factor to analyze the behavior of the system.

3.1. Chemicals

The model water solutions used in the experimentation were prepared by adding salts and metal standards in distilled water combined with sodium chloride. Model water solutions containing lead were prepared using Merck® Pb $(NO_3)_2$, with a purity of 99.5%. Model water solutions containing arsenic were prepared using solutions of 1000 µg/mL from Inorganic Ventures®. The sodium chloride NaCl used was provided by VIOPACK® with a purity of >99%. Membrane cleaning was performed using citric acid from VIOPACK®.

The levels of concentration of the solutions were selected according to the pollutant concentrations found in the previous monitoring of natural waters in the study areas.

Sampling was carried out in compliance with the Bolivian Regulation NB-496, which indicates that wide-mouthed polyethylene bottles should be used, with a 300 mL capacity. A mobile multiparametric equipment HACH model DREL/2088 was used for the conductivity measurements in the different samples. An inductively coupled Perkin Elmer 4300 brand optical emission spectrometer with plasma was used to determine lead and arsenic concentrations.

3.2. Membrane Characteristics and Pilot Plant

The research carried out in the experimental plants installed in Tarija and La Paz for the analysis of lead and arsenic, respectively, used a polyamide spiral-wound membrane module ULP-2540 from Keensem® [55]. The experiments and fitted parameters for the module, such as L_p, σ, k, and $\Delta H/R_g$, were calculated in a particular way based on the experimental results obtained from each study area. The technical characteristics are indicated in Table 1.

Table 1. Technical characteristics of the membrane ULP-2540.

Type:	**Spiral Wound**
Membrane polymer	Composite polyamide
Permeate flow	2.84 m^3/d
Membrane active area	2.5 m^2
Minimum ratio of concentrate	8%
Effective membrane thickness	0.25 µm
Membrane pore diameter	<0.002 µm
Maximum applied pressure	41.4 bar
Maximum operating temperature	45 °C
Maximum feed flow	1.4 m^3/h

Source: [52].

Figure 3 shows the schematic design of the pilot plant assembled for the present work. It consists of a feed water storage tank connected to the centrifugal pump by means of two valves, the pump inlet (V1) and the pump outlet (V2), and a pressure vessel to place a spiral-wound membrane module with pressure gauges at the input feed (M1) and output concentrate (M2). There is a needle-type valve at the exit of the concentrate (V3) to regulate the input flow, and two sensors for the measurement of the permeate (S1) and concentrate flows (S2) with sampling pulses every 6 s. The pump has a frequency regulator which allows the pressure and flow rate to be set with the concentrate valve (V3). Finally, at the outlet of the permeate and concentrate, there are hoses for taking samples.

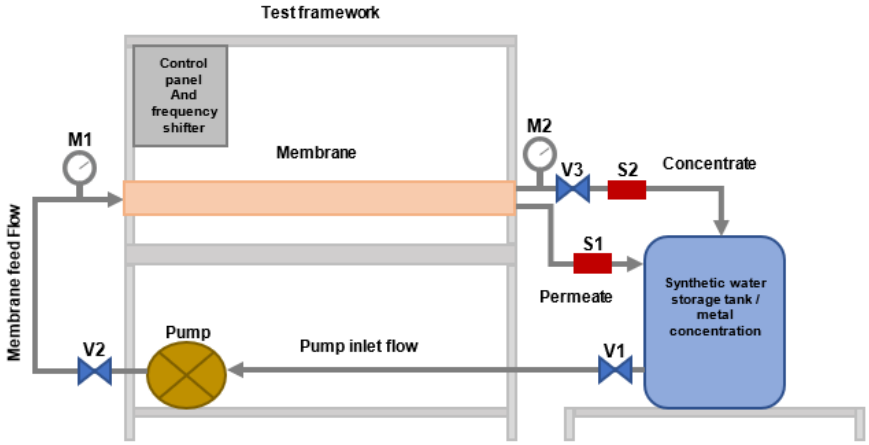

Figure 3. Scheme of the pilot experimental plant for RO [8].

3.3. Design of Experiments and Control Variables

Two different types of experiments were considered according to the tested solutions: (i) solutions containing only the salt of the pollutant (Pb or As), and (ii) solutions containing the pollutant and NaCl to simulate the salinity of the natural waters.

In the design of experiments, the following factors were used: feed pressure, feed flow, and concentration of the solutes. For each factor, three levels (low, medium, high) were used. The plant worked in a closed circuit; nine experimental runs were carried out with average durations of 25 to 30 min each. The selection of concentrations was based on building a model that would allow for the design of installations with high conversion (>80%). With this, it will be possible to optimize the process from the point of view of energy efficiency in future works.

The quality of the water obtained through the monitoring of the main water sources shows that in addition to the presence of Pb and As, they have other contaminants. The presence of these contaminants can generate changes in the behavior of the membrane, so the use of NaCl is defined to simulate the effect of salinity on metal rejection. The use of three levels of solute concentrate in the water is intended to simulate the behavior of the membrane in the face of increased concentrations in the concentrate flow in an industrial design.

Pressure and flow ranges were selected according to the membrane characteristics and levels of concentration to be treated. The experimentation was carried out independently for each pollutant and concentration to evaluate the fouling of the membrane between each concentration of the solute and carry out the respective cleaning before increasing the concentrations. The temperature was used as an adjustment factor.

Model solutions were prepared in quantities of 60 and 50 L for the Tarija and La Paz plants respectively. The composition of the synthetic waters used and the concentration levels are shown in Table 2.

Table 2. Concentrations of solutes in synthetic water.

Solutes	Experimental Concentrations (mol/m^3)		
	C1 (Low)	C2 (Medium)	C3 (High)
Pb	1.5×10^{-04}	1.5×10^{-03}	5.4×10^{-03}
NaCl	3.25	16.3	32.5
AsNaCl	1.44×10^{-04}	4.98×10^{-04}	9.18×10^{-04}
	2.95	15.1	29.7

The low levels reflect the actual concentrations found in the monitoring water. The medium and high concentrations reflect the concentrations in the concentrate flow that might be expected in an industrial-scale design.

The permeation experiments were performed in a total recirculation mode and lasted 25–35 min per run. Samples of the permeate and concentrate were taken to be analyzed. Conductivity was taken as a measure representative of total salinity. An atomic absorption spectrophotometer was used to obtain the final concentrations of Pb or As.

Before each test, the membrane was compacted at a maximum pressure (10 bar) with the corresponding solution for 1 h, without observing significant changes in the flow, since the behavior of the membrane was very stable in all the tests from the first 10 min.

The main experimental runs and the evolution of J_v can be observed in Figures S7–S24 of the Supplementary Materials, where the stabilization time of J_v is observed.

4. Results

The results obtained during the process of separating lead and arsenic combined with sodium chloride in distilled water through a RO process carried out in the two experimental pilot plants are shown.

4.1. Determination of the Dependence of L_p on Temperature

To consider the dependence of permeability with temperature, the Arrhenius adjustment factor was calculated, for which the variation of the flux J_v was recorded at different operating temperatures. Figure 4 shows the regression line of the membrane permeability at a 5-bar pressure for distilled water. The obtained value of the parameter $\Delta H/R$ of Equation (10) was 2459.5 K.

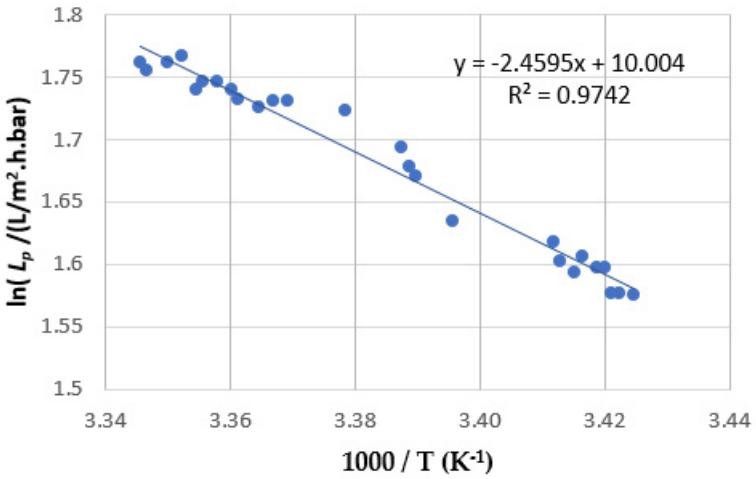

Figure 4. Determination of the membrane permeability temperature adjustment factor for ULP-2540 membrane (P = 5 bar, distilled water).

The figure shows the behavior of the permeate depending on the temperature variation. The parameters allowed us to obtain an adjustment factor applied to the experimental results.

4.2. Effect of Applied Pressure

According to the design of the experiments, the levels established for the working pressures were 5.0, 7.5, and 10 bar. Figures 5 and 6 show the behavior of the experimental flux J_v with respect to the applied pressure ΔP for each pollutant at each concentration level.

The experimental runs were carried out under different water temperatures, starting from an ambient temperature close to 10 °C, and ending close to 30 °C. Flows were normalized to a standard temperature of 25 °C.

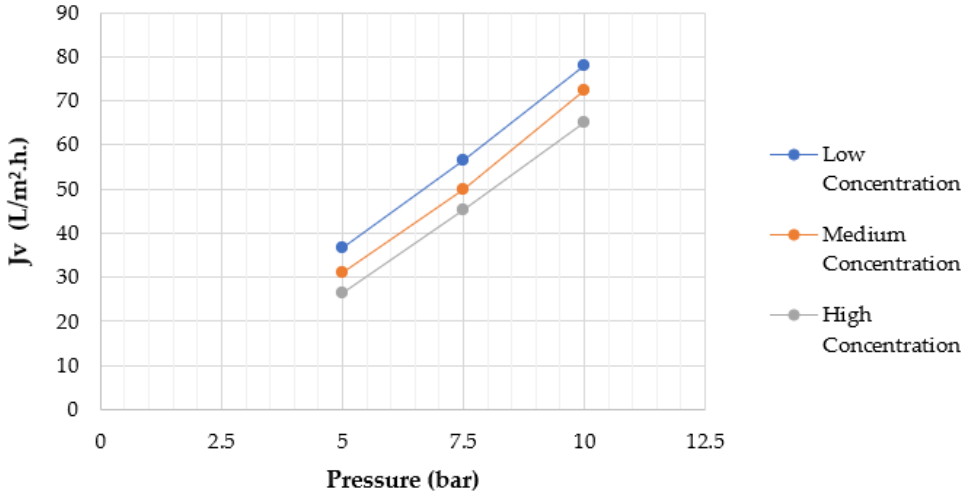

Figure 5. Volumetric flux normalized to 25 °C versus pressure for Pb solutions (ULP-2540).

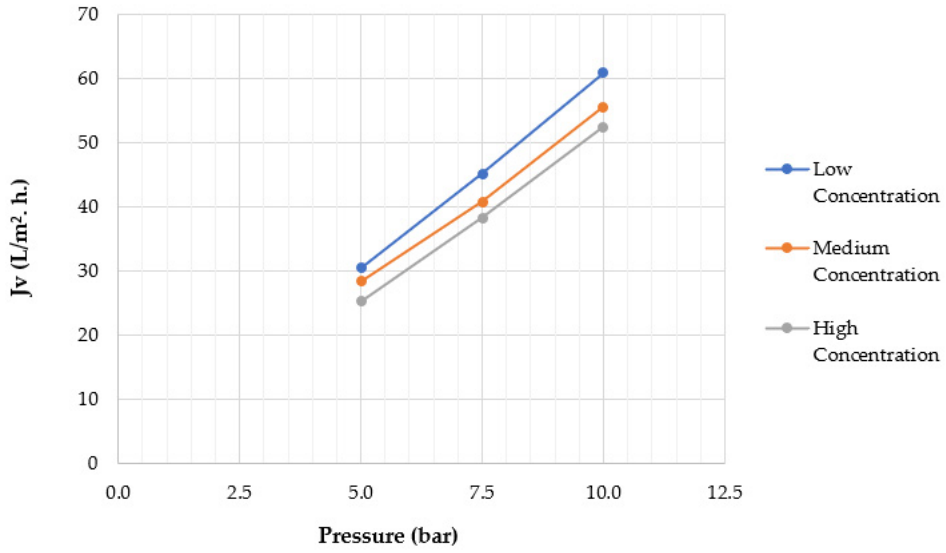

Figure 6. Volumetric flux normalized to 25 °C versus pressure for As solutions (ULP-2540).

For pressure variation, centrifugal pumps with capacities of up to 30 bar were used. In addition, valves were installed at the inlet and outlet of the membrane and a frequency regulator. It is observed in Figures 5 and 6 that with the increase in transmembrane pressure, the J_v increases linearly for the three concentrations. It is also observed that at a higher concentration, the J_v decreases.

Figures 7 and 8 show the observed rejection with respect to the applied pressure for Pb and As solutions, respectively. For solutions containing Pb, the rejection was between 99.0% and 99.4%, with slightly higher rejections at the lower concentration. For solutions containing As, the rejections fell in a range between 99.1% to 99.6%. For both solutions, no significant pressure effect was observed in the pressure range studied. The salt rejection indices obtained in the different operating conditions were high enough to assure permeates with Pb or As concentrations below the permitted limits for water for human consumption.

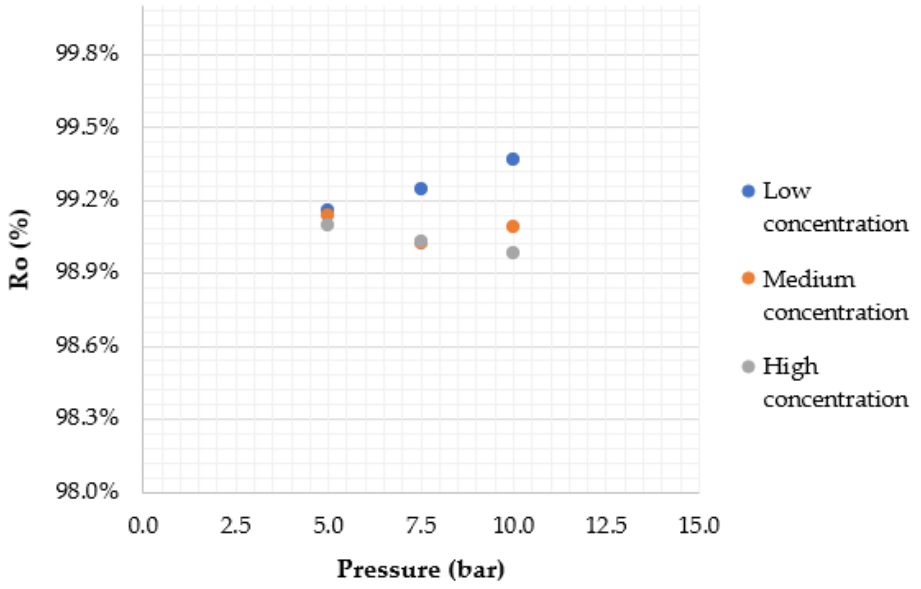

Figure 7. Influence of the applied pressure on Pb salt rejection (feed flow = 0.39 to 0.55 m^3/h, feed concentration = 3.5, 16, and 32 mol/m^3).

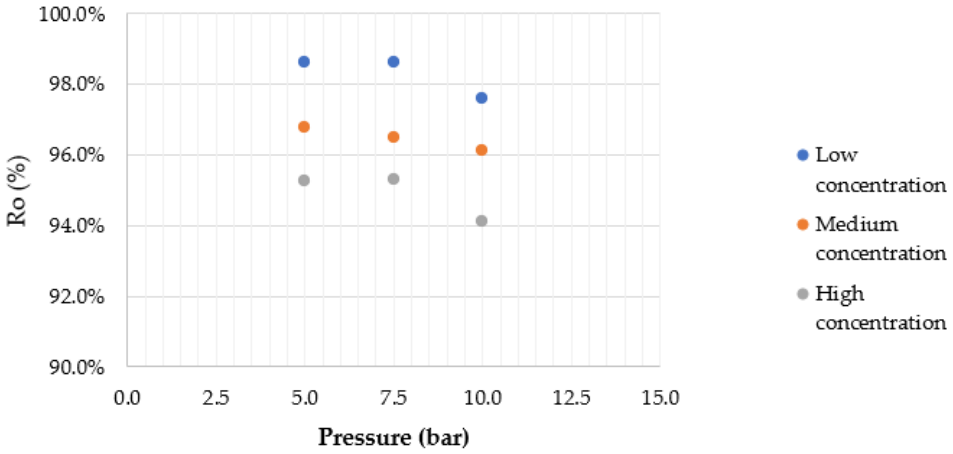

Figure 8. Influence of the applied pressure on As salt rejection (feed flow = 0.29 to 040 m^3/h, feed concentration = 2.9, 15, and 29 mol/m^3).

The results in the rejection are those expected in an RO process. With the investigation, it is evident that with the increase of the input flow, the flow also increases. However, as the concentration increases, the flux decreases. This is explained by the CP phenomenon, which shows that with a lower concentration, the mass is transferred more easily than with higher concentration.

4.3. Effect of Feed Solute Concentration

Figures 9 and 10 show the salt rejection of Pb and As, respectively, for the three composition cases studied. For the Pb solutions, a smaller rejection was observed as the concentration level increased because the increase in the ratio of Pb to NaCl of the membrane produced a decrease in the salt rejection of the solute.

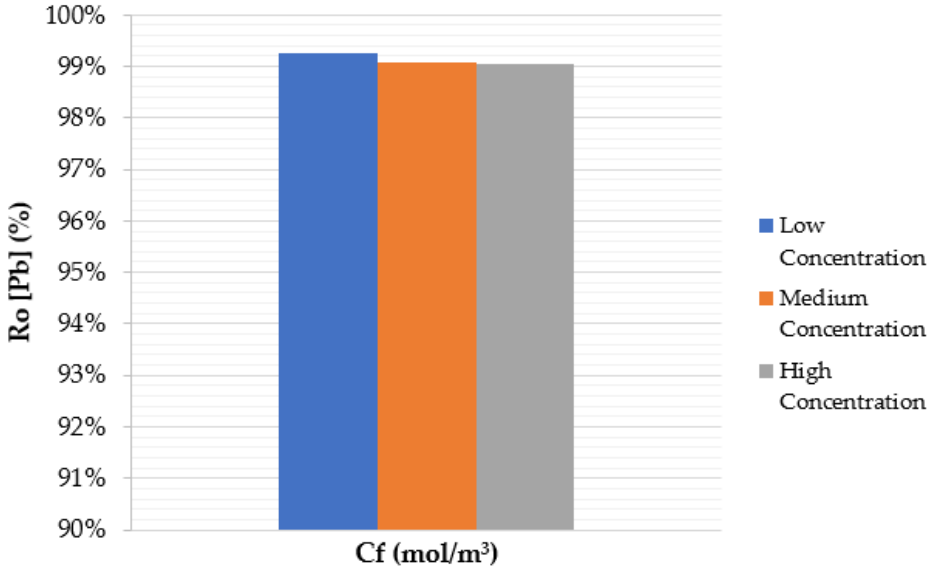

Figure 9. Pb salt rejection for the composition studied.

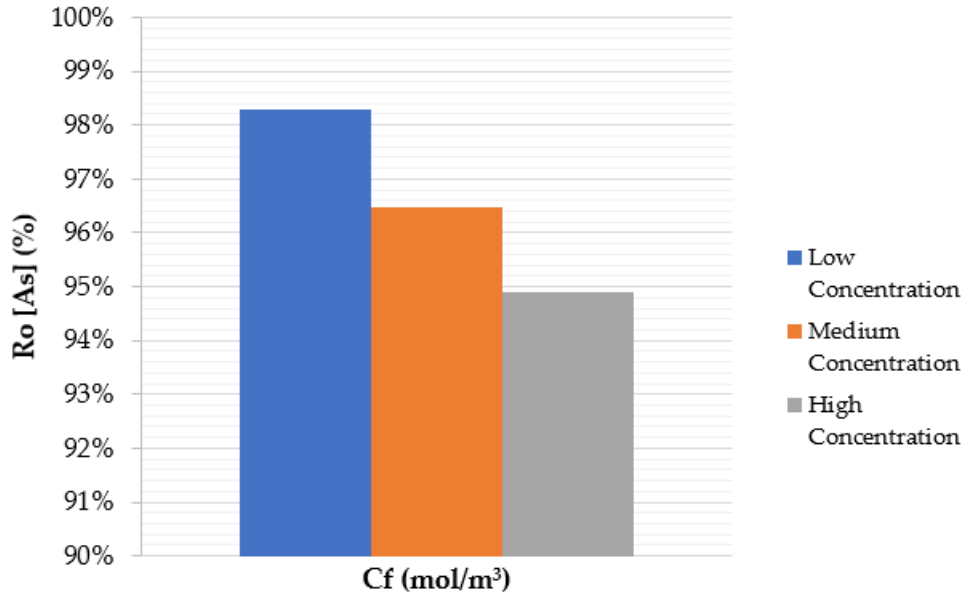

Figure 10. Influence of the Cf on the behavior of salt rejection Ro for As.

In a similar way to the previous graphs, it is observed that at low concentrations the salt rejection was greater, while as the concentration increased, the RO decreased. This was due to the fact that the CP is the phenomenon that governs the process. Lead shows a more similar trend compared to arsenic showing a marked difference in rejection.

4.4. Model Validation

For the validation process of the model, the reflection coefficients σ were first estimated for the operation of the system. The results for each metal and concentration are shown in Table 3. The calculation was performed using the Matlab [56] curve fitting application from the experimental results obtained in the different concentrations.

Table 3. Calculation of reflection coefficients.

Pollutants	Concentration	σ (Metal + NaCl)
Lead (Pb)	Low	0.9900
	Medium	0.9917
	High	0.9921
Arsenic (As)	Low	0.9935
	Medium	0.989
	High	0.9912

The calculation of non-linear parameters such as the hydraulic permeability constant Lp and the mass transfer coefficient k are shown in Tables 4 and 5 for the metal + NaCl combinations of the different concentrations. Similar to the research found in [29], the CP theory allowed us to simultaneously determine and evaluate the three detailed parameters.

Table 4. Calculation of non-linear parameters of the model by concentrations for the Pb.

Concentration	Metal	σ	Lp (L/m^2.h.bar)	k (m/s)
		Metal + NaCl	Metal + NaCl	Metal + NaCl
Low	Pb	0.990	6.714	1.15×10^{-05}
Medium	Pb	0.9917	6.1114	51.56×10^{-04}
High	Pb	0.9921	5.5901	69.45×10^{-04}

Table 5. Calculation of non-linear parameters of the model by concentrations for the As.

Concentration	Metal	σ	Lp (L/m^2.h.bar)	k (m/s)
		Metal + NaCl	Metal + NaCl	Metal + NaCl
Low	As	0.9935	6.198	5.6×10^{-06}
Medium	As	0.989	7.618	5.83×10^{-06}
High	As	0.9912	6.855	7.49×10^{-06}

The flow rates of permeate Qp and concentrate Qs have been measured with a flow sensor installed at the outlet of the permeate and concentrate. This has allowed the calculation of the entrance flow Qf and the experimental J_v. With the parameters calculated and detailed in Tables 4 and 5 and using Equations (10) and (11), the J_v (theoretical) was calculated. The behavior of the model is illustrated in Figures 11–13 for lead and Figures 14–16 for arsenic. In the Supplementary Material are the Matlab scripts S.1.1 to S.6.2, for the evaluation and validation of the model.

The main operating conditions that caused the three steps in the figure are the transmembrane pressure that varied between 5.0, 7.5, and 10 bar. The variation of J_v is influenced by the concentrations of the solute, represented in each figure.

The figures show an adequate fit of the model for the behavior of lead. The maximum differences between the theoretical and experimental values were 3.0% and 5.4%, which were generated in the medium and high concentrations. This is expected in the effect of CP, considering that the fluxes decrease when the concentrations increase.

In the case of arsenic, the maximum difference between the theoretical and experimental values were 4.4% and 3.6%, and the medium concentration was the one that shows the greatest difference.

Graphs 17 and 18 detail the maximum errors between the experimental and theoretical values for lead and arsenic, obtained from the validation of the model.

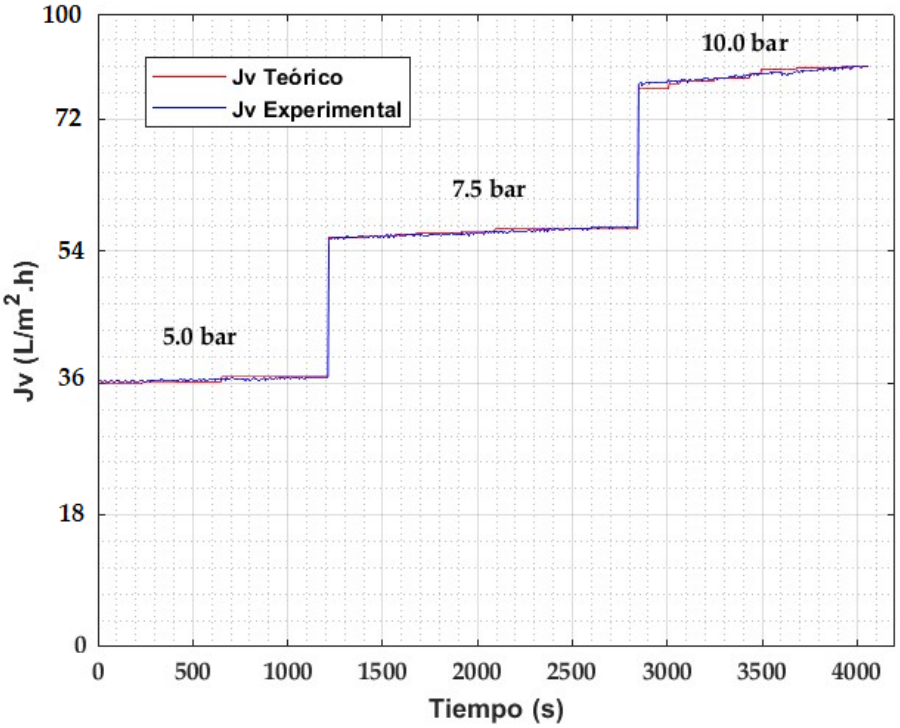

Figure 11. Theoretical vs. experimental flux of Pb: low concentration.

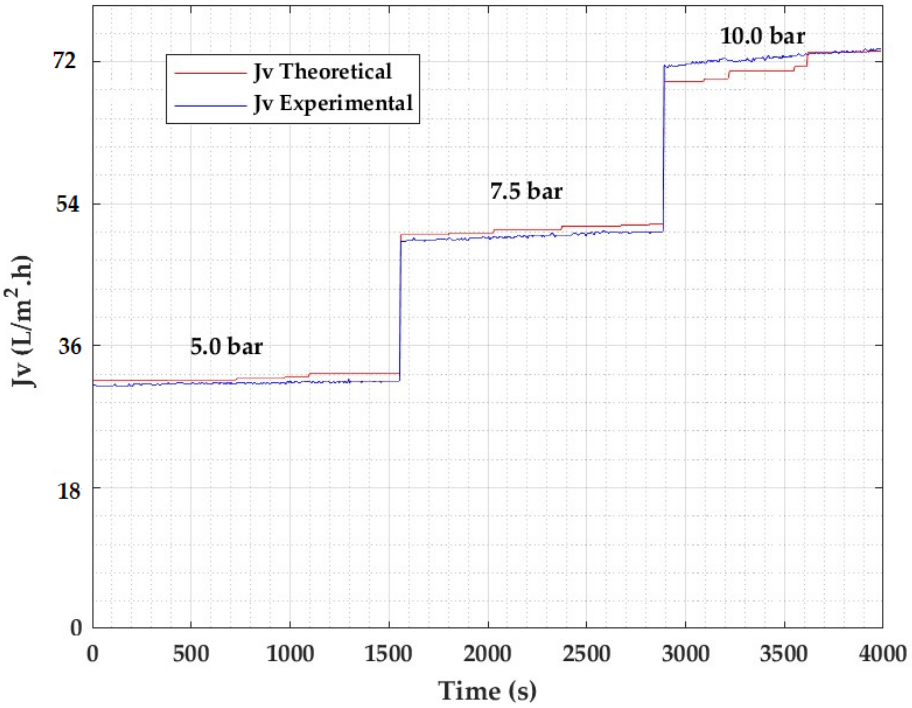

Figure 12. Theoretical vs. experimental flux of Pb: medium concentration.

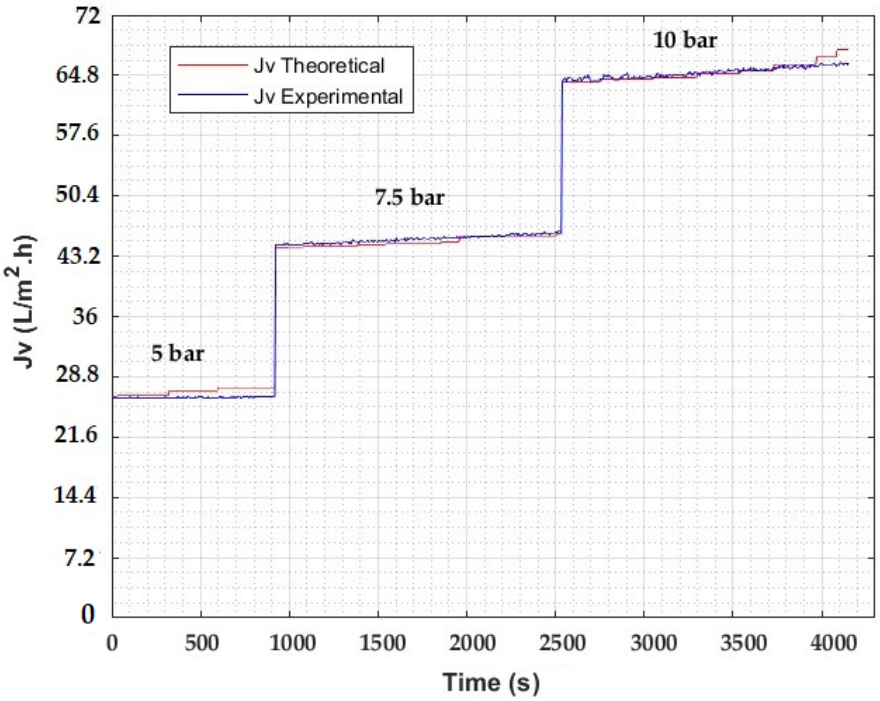

Figure 13. Theoretical vs. experimental flux of Pb: high concentration.

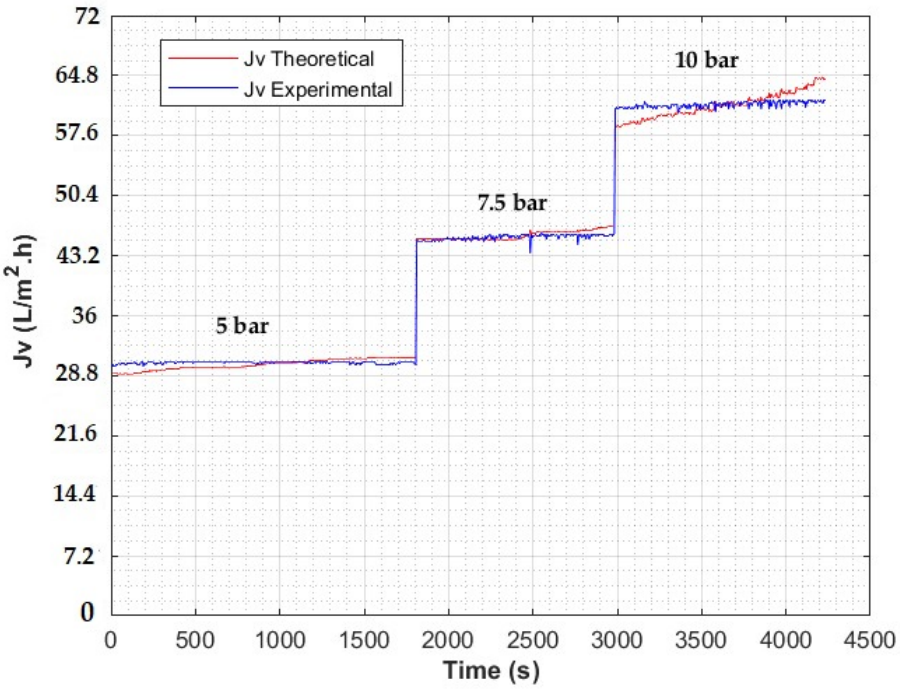

Figure 14. Theoretical vs. experimental flux of As: low concentration.

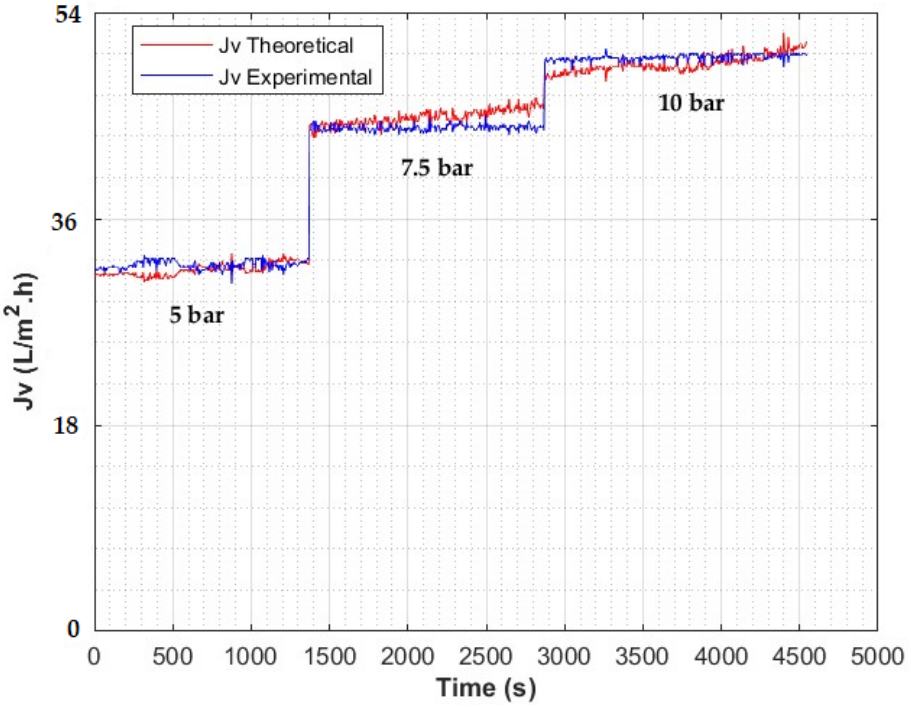

Figure 15. Theoretical vs. experimental flux of As: medium concentration.

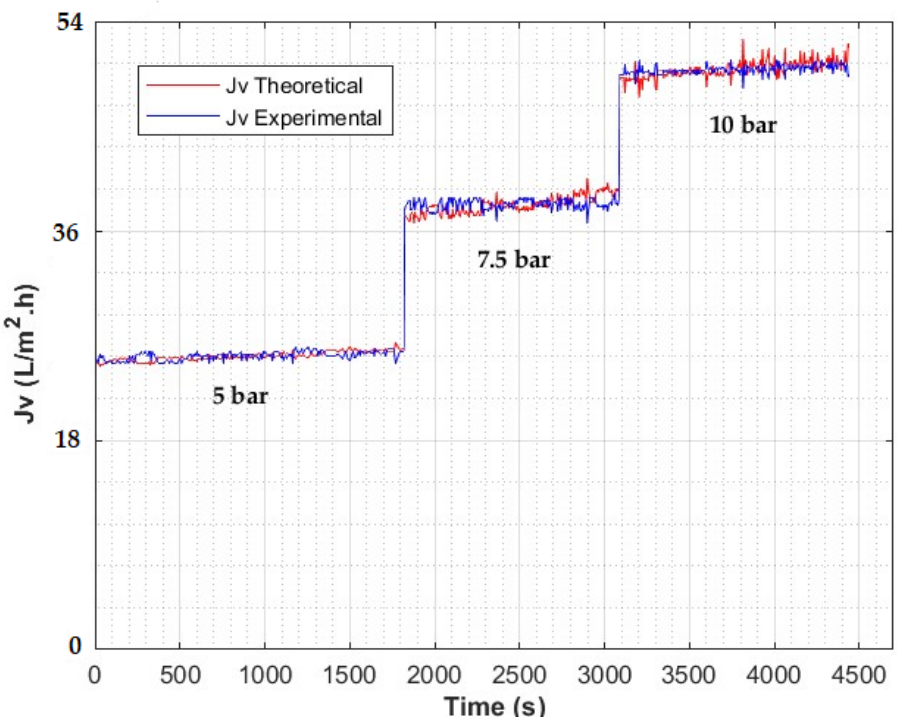

Figure 16. Theoretical vs. experimental flux of As: high concentration.

Figures 11–16 show the validation of the model through the theoretical vs. experimental behavior of the system, and the three steps show the behavior of the metal with the three concentrations analyzed. The time reflects the average duration of the experiment that was needed to reach stabilization of the flows. Figures 17 and 18 show the maximum relative errors between the theoretical and experimental J_v found in the validation. For both metals they were generated at high concentrations and with high pressures.

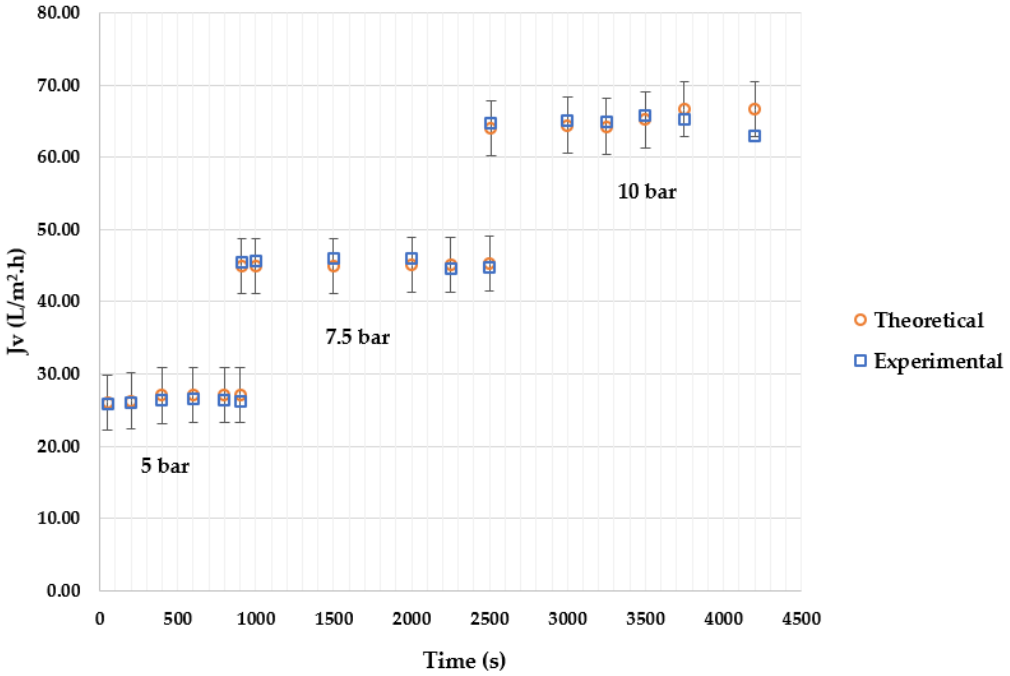

Figure 17. Theoretical vs. experimental Pb comparison: maximum error at high concentration.

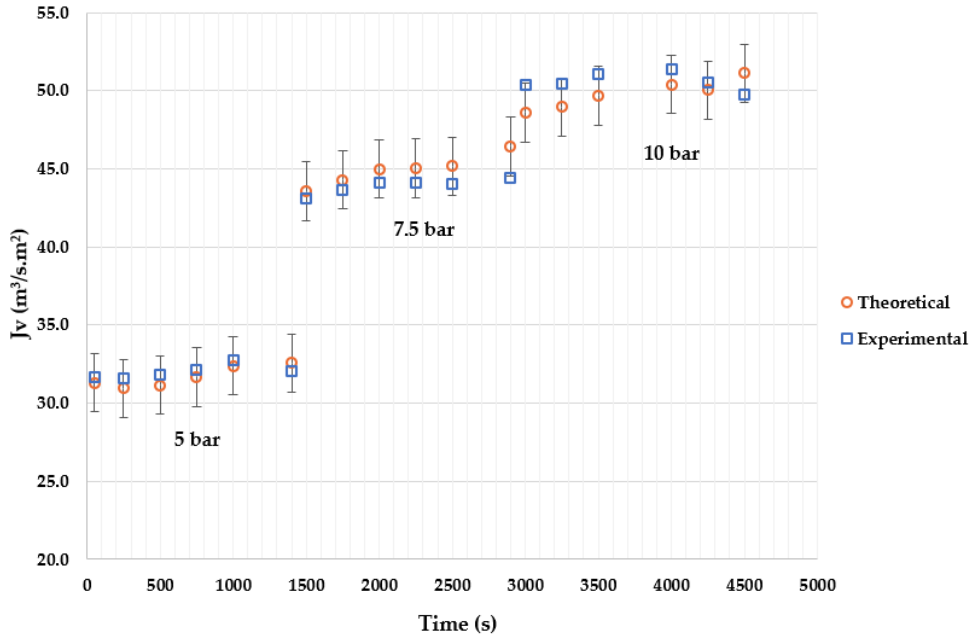

Figure 18. Theoretical vs. experimental As comparison: maximum error at high concentration.

The temperature correction included in the model allows for an adequate adjustment of it. This is observed in the calculated theoretical flow, which shows a clear increasing trend, which is normal in the separation process as the temperature of the solution increases. The foregoing exposes a congruence between the experimental and theoretical behavior, validating the proposed model.

The graphs of the experimental flux with respect to the theoretical J_v allowed us to establish an adequate behavior of the separation model of metals with relative errors between the two not greater than 5.4% for lead and 4.4% for arsenic.

The design of the experiments and the experimental tests were carried out to verify and evaluate the flux over time, and the validation of the model illustrated in Figures 11–16.

The experiments considered the pH during the experimental process. It varied between 5.72 and 7.45 for lead and 6.72 and 7.18 for arsenic. The variations were due to the variation in the concentrations of the Pb, As, and NaCl salts used in the synthetic waters.

4.5. Discussion of Results

Although the temperature is a natural variable, it cannot be controlled like other plant operating parameters. During the experimentation, the permeability in solute (Pb, As, and NaCl) transport followed an Arrhenius type of relationship as indicated by Mulder et al. [38]. This made it possible to evaluate the effect of temperature on the operation of reverse osmosis, as indicated by Lora et al. [37].

It is observed that the recovery of water improves with the increase in the feeding pressure and temperature, but decreases with increasing metal concentration. This is in agreement with the study presented by Alanood et al. [39]

The results show that the Pb and As rejections decrease as the concentration level increases. These results agree with the work of Pontié et al. [54], who present an approach that combines the characterization and modeling of mass transfer in a low-pressure RO system.

The mathematical model for the separation of metals such as Pb and As in water by reverse osmosis (RO) made it possible to investigate the behavior of the membrane during the mass transfer process. The validation of the model was carried out using experimental results that show low relative errors between the experimental and theoretical results, similarly to the research conducted by Chenghan and Han [16].

4.6. Energetic Reflexions

The model shows that the rejection rates obtained for Pb and As can be operated at low operating pressures. These considerations have an important impact on economic and health aspects.

The problem of heavy metals in surface water denotes a risk to global public health. However, the economic factor that is directly related to the applicability of different technologies to remove metal ions from water cannot be ignored. In this sense, the current challenge is to develop or optimize processes, such as reverse osmosis, to make it eco-efficient, and thus achieve sustainability within the process. This would guarantee a greater implementation of reverse osmosis technology in developing countries. This study coincides with the research by [39] that indicates that lower energy consumption can be achieved with lower values of flow and pressures.

5. Conclusions

The experimental process carried out using the two pilot plants shows that RO systems are efficient in rejecting Pb and As in drinking water from the Guadalquivir–Tarija and Milluni–La Paz basins, achieving rejection rates close to 99%.

A mathematical model based on Spiegler and the Kedem Polarization Concentration was developed, which allowed for the evaluation of the process and the analysis of the physical behavior of a polyamide membrane with a spiral configuration.

The model was developed including an Arrhenius temperature adjustment factor, allowing for an accurate prediction of process performance.

The results show that at low pressures and metal concentrations, the behavior of the flux is linear, and the membrane does not present physical compaction. On the other hand, at high concentrations, the flow has a different behavior due to the difficulty in the process of mass transfer by CP near the membrane surface.

It was also evidenced that with the increase of the input flux, the flux also increases. However, as the concentration increases, the flux decreases. This is explained by the CP phenomenon; that is, at a lower concentration, the mass is more easily transferred than at a higher concentration due to the lower CP phenomenon.

The validation of the model showed that the maximum relative errors between the theoretical J_v and the experimental J_v in Pb occur with high concentrations and pressures,

reaching a 5.4% error. In the case of As, similar behavior was observed with maximum errors of 4.4%.

The selection of the concentrations allowed us to build a model that allows the design of installations with high conversion (>80%). With this, it will be possible to optimize the process from the point of view of energy efficiency in future works.

The operating conditions of the experimental process such as pressure, the concentration of pollutants, and temperature effects, and the results obtained in the rejection of Pb and As, show that an industrial design can be developed in the future in the study basins with energy-efficiency and economic and sustainable operating processes.

Supplementary Materials: The following supporting information can be downloaded at: https://www.mdpi.com/article/10.3390/pr10091889/s1. The evaluation of the three lead concentrations is detailed in the Matlab Calculation Scripts S.1.1, S.1.2, S.2.1, S.2.2, S.3.1 and S.3.2. For Arsenic the Scripts are S.4.1, S.4.2, S.5.1, S.5.2, S.6.1 and S.6.2. The behavior and evolution of J_v for Pb are detailed in Figures S7–S15 and for As, Figures S16–S24.

Author Contributions: E.M.V.-M.: Investigation, Conceptualization, Methodology, Software, Data curation, Writing—Original draft preparation. P.A.A.-T.: Investigation, Conceptualization, Methodology, Software, Writing—Original draft preparation, Writing—Review and Editing. J.L.-G.: Data curation, Investigation, Data curation, Formal analysis, Validation. J.I.T.-L.: Project administration, Funding acquisition. V.G.L.-I.-F.: Visualization, Supervision, Writing Review and Editing. All authors have read and agreed to the published version of the manuscript.

Funding: This work was supported by the Universidad Católica Boliviana "San Pablo"—Academic Units of La Paz and Tarija, and by the Universitat Politècnica de Valencia through the ADSIDEO project.

Institutional Review Board Statement: Not applicable.

Informed Consent Statement: Not applicable.

Data Availability Statement: Not applicable.

Acknowledgments: The authors appreciate the support of the national and regional authorities of the Universidad Católica Boliviana "San Pablo". The research was carried out with the support of the Department of Engineering and Exact Sciences of the Universidad Católica Boliviana headquarters in Tarija, and the Center for Research in Water, Energy, and Sustainability (CINAES) of the Environmental Engineering career of the Bolivian Catholic University "San Pablo" headquarters in La Paz. A special thanks to José Gozálvez Zafrilla for the important support in this research.

Conflicts of Interest: The authors declare that they have no known competing financial interests or personal relationships that could have appeared to influence the work reported in this paper.

References

1. Chen, L.; Zhang, X.; Cao, M.; Pan, Y.; Xiao, C.; Wang, P.; Liang, Y.; Liu, G.; Cai, Y. Release of legacy mercury and effect of aquaculture on mercury biogeochemical cycling in highly polluted Ya-Er Lake, China. *Chemosphere* **2021**, *275*, e130011. [CrossRef]
2. Mora, A.; García-Gamboa, M.; Sánchez-Luna, M.S.; Gloria-García, L.; Cervantes-Avilés, P.; Mahlknecht, J. A review of the current environmental status and human health implications of one of the most polluted rivers of Mexico: The Atoyac River, Puebla. *Sci. Total Environ.* **2021**, *782*, e146788. [CrossRef]
3. Runkel, A.A.; Križanec, B.; Lipičar, E.; Baskar, M.; Hrženjak, V.; Kodba, Z.C.; Kononenko, L.; Kanduč, T.; Mazej, D.; Tratnik, J.S.; et al. Organohalogens: A persisting burden in Slovenia? *Environ. Res.* **2021**, *198*, e111224. [CrossRef]
4. Garrido, A.E.; Strosnider, W.H.; Wilson, R.T.; Condori, J.; Nairn, R.W. Metal-contaminated potato crops and potential human health risk in Bolivian mining highlands. Environ. Geochem. *Health* **2017**, *39*, 681–700. [CrossRef]
5. Quaghebeur, W.; Mulhern, R.E.; Ronsse, S.; Heylen, S.; Blommaert, H.; Potemans, S.; Valdivia Mendizábal, C.; Terrazas García, J. Arsenic contamination in rainwater harvesting tanks around Lake Poopó in Oruro, Bolivia: An unrecognized health risk. *Sci. Total Environ.* **2019**, *688*, 224–230. [CrossRef] [PubMed]
6. Salvarredy-Aranguren, M.M.; Probst, A.; Roulet, M.; Isaure, M.-P. Contamination of surface waters by mining wastes in the Milluni Valley (Cordillera Real, Bolivia). Mineralogical and hydrological influences. *Appl. Geochem.* **2008**, *23*, 1299–1324.e5. [CrossRef]

7. Alvizuri, P.A.; Torregrosa, J.I.; Lo Iacono, V.G.; Salinas, O.R. Heavy metals problem in micro-basin that feeds a drinking water dam, Milluni-Bolivia case. In Proceedings of the XXIII International Congress on Project Management and Engineering, Málaga, Spain, 10–12 July 2019; pp. 1059–1071. Available online: http://dspace.aeipro.com/xmlui/handle/123456789/2396 (accessed on 12 June 2022).
8. Villena, E.; Alvizuri, P.; Torregrosa, J.; Lo Iacono, V.; Lora, J. Diseño y Montaje de una Planta Experimental Piloto de Ósmosis Inversa para la Remoción de Metales Pesados Pb, Fe, As, Zn y Mn en aguas de consumo humano. In Proceedings of the 24th International Congress on Project Management and Engineering, Alcoi, Spain, 7–10 July 2020; pp. 1252–1264. Available online: http://dspace.aeipro.com/xmlui/handle/123456789/2509 (accessed on 12 June 2022).
9. Gumucio Dagrón, A.; Elemento de vida: El agua en el desarrollo, la cultura y la Sociedad. Journal of Swiss cooperation in Bolivia 2016–2017. Available online: https://ibce.org.bo/publicaciones-descarga.php?id=2394 (accessed on 12 June 2022).
10. Medina, I.; Smolders, A.; Lebrato, J.; Coronel, F.; Orozco, M. Contaminación De La Represa De San Jacinto (Tarija, Bolivia) Interpretación Del Informe Técnico De La Unam. Available online: https://sihita.org/wp-content/uploads/2022/03/DOC069.pdf (accessed on 12 June 2022).
11. Zak, S. Treatment of the processing wastewaters containing heavy metals with the method based on flotation. *Ecol. Chem. Eng.* **2012**, *19*, 433–438. [CrossRef]
12. Abdullah, N.; Yusof, N.; Lau, W.J.; Jaafar, J.; Ismail, A.F. Recent trends of heavy metal removal from water/wastewater by membrane technologies. *J. Ind. Eng. Chem.* **2019**, *76*, 17–38. [CrossRef]
13. Atab, M.; Smallbone, A.; Roskilly, A. A hybrid reverse osmosis/adsorption desalination plant for irrigation and drinking water. *Desalination* **2018**, *444*, 44–52. [CrossRef]
14. Kim, S.; Chu, K.H.; Al-Hamadani, Y.A.; Park, C.M.; Jang, M.; Kim, D.H.; Yu, M.; Heo, J.; Yoon, Y. Removal of contaminants of emerging concern by membranes in water and wastewater: A review. *Chem. Eng. J.* **2018**, *335*, 896–914. [CrossRef]
15. Ray, S.; Chen, S.; Sangeetha, D.; Chang, H.; Thanh, C.; Le, Q.; Ku, H. Developments in forward osmosis and membrane distillation for desalination of waters. *Environ. Chem. Lett.* **2018**, *16*, 1247–1265. [CrossRef]
16. Chenghan, C.; Han, Q. A Mathematical Modeling of the Reverse Osmosis Concentration Process of a Glucose Solution. *Processes* **2019**, *7*, 271. [CrossRef]
17. Chung, T.; Zhang, S.; Wang, K.; Su, J.; Ling, M. Forward osmosis processes: Yesterday, today and tomorrow. *Desalination* **2012**, *287*, 78–81. [CrossRef]
18. Khulbe, K.C.; Matsuura, T. Removal of heavy metals and pollutants by membrane adsorption techniques. *Appl. Water Sci.* **2018**, *8*, 19. [CrossRef]
19. Ray, S.; Chen, S.; Nguyen, N.; Nguyen, H.; Dan, N.; Thanh, B. Exploration of polyelectrolyte incorporated with Triton-X 114 surfactant based osmotic agent for forward osmosis desalination. *J. Environ. Manag.* **2018**, *209*, 346–353. [CrossRef] [PubMed]
20. Saravanan, A.; Senthil Kumar, P.; Jeevanantham, S.; Karishma, S.; Tajsabreen, B.; Yaashikaa, P.R.; Reshma, B. Effective water/wastewater treatment methodologies for toxic pollutants removal: Processes and applications towards sustainable development. *Chemosphere* **2021**, *280*, 130595. [CrossRef] [PubMed]
21. Fritzmann, C.; Löwenberg, J.; Wintgens, T.; Melin, T. State-of-the-art of reverse osmosis desalination. *Desalination* **2007**, *216*, 1–76. [CrossRef]
22. Sablani, S.S.; Goosen, M.F.A.; Al-Belushi, R.; Wilf, M. Concentration polarization in ultrafiltration and reverse osmosis: A critical review. *Desalination* **2001**, *141*, 269–289. [CrossRef]
23. Wei, W.; Zou, X.; Ji, X.; Zhou, R.; Zhao, K.; Wang, Y. Analysis of Concentration Polarisation in Full-Size Spiral Wound Reverse Osmosis Membranes Using Computational Fluid Dynamics. *Membranes* **2021**, *11*, 353. [CrossRef]
24. Qasim, M.; Badrelzaman, M.; Darwish, N.N.; Darwish, N.A.; Hilal, N. Reverse osmosis desalination: A state-of-the-art review. *Desalination* **2019**, *459*, 59–104. [CrossRef]
25. Salcedo, R.; Aplicación de la Interferometría Holográfica al Estudio de la Capa de Polarización en Ósmosis Inversa. Efecto de la Convección Natural. *Tesis Doctoral Universidad de Alicante. España.* 2006. Available online: https://dialnet.unirioja.es/servlet/tesis?codigo=68704 (accessed on 12 June 2022).
26. Feria-Díaz, J.J.; Correa-Mahecha, F.; López-Méndez, M.C.; Rodríguez-Miranda, J.P.; Barrera-Rojas, J. Recent Desalination Technologies by Hybridization and Integration with Reverse Osmosis: A Review. *Water* **2021**, *13*, 1369. [CrossRef]
27. Fariñas, M.; Osmosis Inversa. Fundamentos Tecnología y aplicaciones. Mc GrawHill, Ente Vasco de la Ingeniería, EVE, e IBERDROLA, España. 1999, pp. 163–168. Available online: https://dialnet.unirioja.es/servlet/libro?codigo=34001 (accessed on 12 June 2022).
28. García, C. Aplicación de Ósmosis Inversa y Nanofiltración en Acondicionamiento de Agua Para Calderas. Ph.D Thesis, Universidad de Oviedo, Oviedo, Spain, 2002. Available online: https://www.tesisenred.net/handle/10803/11146 (accessed on 12 June 2022).
29. Aramijo, C.; Condorhuaman, C. Simulación dinámica de sistemas de osmosis inversa. *Rev. Per. Quim. Ing. Química.* **2012**, *15*, 21–34. Available online: https://revistasinvestigacion.unmsm.edu.pe/index.php/quim/article/view/4758/3831 (accessed on 12 June 2022).
30. Sundaramoorthy, S.; Srinivasan, G.; Murthy, D. An analytical model for spiral wound reverse osmosis membrane modules: Part I—Model development and parameter estimation. *Desalination* **2011**, *280*, 403–411. [CrossRef]

31. AlSawaftah, N.; Abuwatfa, W.; Darwish, N.; Husseini, G. A Comprehensive Review on Membrane Fouling: Mathematical Modelling, Prediction, Diagnosis, and Mitigation. *Water* **2021**, *13*, 1327. [CrossRef]
32. Gu, B.; Adjiman, C.S.; Xu, X.Y. Correlations for Concentration Polarization and Pressure Drop in Spacer-Filled RO Membrane Modules Based on CFD Simulations. *Membranes* **2021**, *11*, 338. [CrossRef] [PubMed]
33. Salcedo, R.; García-Algado, P.; García-Rodríguez, M.; Fernández-Sempere, J.; Ruiz-Beviá, F. Visualization and modeling of the polarization layer in crossflow reverse osmosis in a slit-type channel. *J. Membr. Sci.* **2014**, *456*, 21–30. [CrossRef]
34. Khalaf, T. Estimation of Concentration Polarization Using the Combined Film theory/Spiegler-Kedem Model and Empirical Correlation. *Al-Nahrain J. Eng. Sci.* **2008**, *11*, 322–328. Available online: https://nahje.com/index.php/main/article/view/527 (accessed on 12 June 2022).
35. Otero-Fernández, A.; Otero, J.A.; Maroto, A.; Carmona, J.; Palacio, L.; Prádanos, P.; Hernández, A. Concentration-polarization in nanofiltration of low concentrationCr(VI) aqueous solutions. Effect of operative conditions on retention. *J. Clean. Prod.* **2017**, *150*, 243–252. [CrossRef]
36. Al-Obaidi, M.A.; Kara-Zaïtri, C.; Mujtaba, I.M. Wastewater treatment by spiral wound reverse osmosis: Development and validation of a two dimensional process model. *J. Clean. Prod.* **2017**, *140*, 1429–1443. [CrossRef]
37. Lora, J.; López, M.; Cardona, S.; Fombuena, V.; Carbonell, A. Análisis del consumo Energético como factor clave en proyectos de desalación de agua de mar. In Proceedings of the 24th International Congress on Project Management and Engineering, Alcoi, Spain, 7–10 July 2020; pp. 991–1003. Available online: http://dspace.aeipro.com/xmlui/handle/123456789/2486 (accessed on 12 June 2022).
38. Mulder, M. *Basic Principles of Membrane Technology*; Springer Science & Business Media: Berlin/Heidelberg, Germany, 1996; pp. 246–248, 281–304. Available online: https://ebookcentral.proquest.com/lib/bibliotecaupves-ebooks/reader.action?docID=3102158&ppg=1 (accessed on 12 June 2022).
39. Alanood, A.; Al-Obajdib, M.A.; Al-Hroubc, A.M.; Patela, R.; Mujtaba, I.M. Evaluation and minimisation of energy consumption in a mediumscale reverse osmosis brackish water desalination plant. *J. Clean. Prod.* **2020**, *248*, 119220. [CrossRef]
40. Abejón, A.; Garea, A.; Irabién, A. Arsenic removal from drinking water by reverse osmosis: Minimization of costs and energy consumption. *Sep. Purif. Technol.* **2015**, *144*, 46–53. [CrossRef]
41. Ning, R. Arsenic removal by reverse osmosis. *Desalination* **2002**, *143*, 237–241. [CrossRef]
42. Schimdt, A.; Gukelberger, E.; Hermann, M.; Fiedler, F.; Großmann, B.; Hoinkins, J.; Ghosh, A.; Chatterjee, D.; Bundschuh, J. Pilot study on arsenic removal from groundwater using a small-scale reverse osmosis system—Towards sustainable drinking water production. *J. Hazard. Mater.* **2016**, *318*, 671–678. [CrossRef]
43. Moreira, V.R.; Lebron, Y.A.R.; de Paula, E.C.; de Souza Santos, L.V.; Amaral, M.C.S. Recycled reverse osmosis membrane combined with pre-oxidation for improved arsenic removal from high turbidity waters and retrofit of conventional drinking water treatment process. *J. Clean. Prod.* **2021**, *312*, 127859. [CrossRef]
44. Walker, M.; Seiler, R.L.; Meinert, M. Effectiveness of household reverse-osmosis systems in a Western US region with high arsenic in groundwater. *Sci. Total Environ.* **2008**, *389*, 245–252. [CrossRef]
45. Tang, C.Y.; Reinhard, M.; Leckie, J.O. Effects of hypochlorous acid exposure on the rejection of salt, polyethylene glycols, boron and arsenic (V) by nanofiltration and reverse osmosis membranes. *Water Res.* **2012**, *46*, 5217–5223.
46. Li, Y.; Xu, Z.; Liu, S.; Zhang, J.; Yang, X. Molecular simulation of reverse osmosis for heavy metal ions using functionalized nanoporous graphenes. *Comput. Mater. Sci.* **2017**, *139*, 65–74. [CrossRef]
47. Schneiter, R.W.; Middlebrooks, E.J. Arsenic and fluoride removal from groundwater by reverse osmosis. *Environ. Int.* **1983**, *9*, 289–291. [CrossRef]
48. Kang, M.; Kawasaki, M.; Tamada, S.; Kamei, T.; Magara, Y. Effect of pH on the removal of arsenic and antimony using reverse osmosis membranes. *Desalination* **2000**, *131*, 293–298. [CrossRef]
49. Akin, I.; Arslan, G.; Tor, A.; Cengeloglu, Y.; Ersoz, M. Removal of arsenate [As(V)] and arsenite [As(III)] from water by SWHR and BW-30 reverse osmosis. *Desalination* **2011**, *281*, 88–92. [CrossRef]
50. Spiegler, K.; Katchalsky, A. *Permeability of Composite Membranes Part 1—Electric Current, Volume Flow and Flow of Solute through Membranes*; Instituto de Ciencias Weizmann: Rehovot, Israel, 1963; Volume 59, pp. 1918–1930.
51. Spiegler, K.; Kedem, O. Thermodynamics of hyperfiltration (reverse osmosis): Criteria for efficient membranes. *Desalination* **1966**, *1*, 311–326. [CrossRef]
52. Alvizuri-Tintaya, P.A.; Villena Martínez, M.E.; Torregrosa López, J.I.; Lo-Iacono-Ferreira, V.G.; Lora, J. Review of membrane technologies in the removal of heavy metals in surface waters for human consumption. In Proceedings of the XXIV International Congress on Project Management and Engineering, Alcoy, Spain, 7–10 July 2020; pp. 1130–1141. Available online: http://dspace.aeipro.com/xmlui/handle/123456789/2498 (accessed on 12 June 2022).
53. NB512. Norma Boliviana 512-Agua potable y Requisitos. 2022. Available online: http://www.anesapa.org/data/files/NB512-AP_Requisitos.pdf (accessed on 12 June 2022).
54. Pontié, M.; Dach, H.; Leparc, J.; Hafsi, M.; Lhassani, A. Novel approach combining physico-chemical characterizations and mass transfer modelling of nanofiltration and low-pressure reverse osmosis membranes for brackish water desalination intensification. *Desalination* **2008**, *221*, 174–191. [CrossRef]
55. Kennsen. 2020. Available online: http://www.keensen.com/Products/ultralowpressur.html (accessed on 12 June 2022).
56. Matlab, 2021. MathWorks. Version R2021a.